Soft Matter

PAPER

Cite this: *Soft Matter*, 2020, **16**, 7556

Microrheology to probe smectic clusters in bent-core nematic liquid crystals†

Sathyanarayana Paladugu, *[ab] Supreet Kaur, [c] Golam Mohiuddin, [c] Ravi Kumar Pujala, [b] Santanu Kumar Pal [c] and Surajit Dhara *[a]

Received 2nd May 2020,
Accepted 1st July 2020

DOI: 10.1039/d0sm00796j

rsc.li/soft-matter-journal

Many bent-core nematic liquid crystals exhibit unusual physical properties due to the presence of smectic clusters, known as "cybotactic" clusters, in the nematic phase. Here, we investigate the effect of these clusters on the complex shear modulus ($G^*(\omega)$) of two asymmetric bent-core liquid crystals using a microrheological technique. The compound with a shorter hydrocarbon chain ($8OCH_3$) exhibits only a nematic (N) phase whereas the compound with a longer chain ($16OCH_3$) exhibits both nematic (N) and smectic-A (SmA) phases. The rheological results are correlated with the measurements of curvature elastic constants. Our results show that the directional shear modulus of $16OCH_3$, just above the SmA to N phase transition temperature, is strikingly different than that of $8OCH_3$, owing to the smectic clusters. An approximate size of the clusters is estimated using a simple model. Therefore, microrheological studies on bent-core nematic liquid crystals are very useful in extracting information about underlying smectic clusters.

1 Introduction

Bent-core (BC) liquid crystals have captivated the interest of many scientists as they continue to exhibit new and interesting physical properties compared to conventional calamitic liquid crystals made of rod-like molecules.[1,2] For example, bent-core nematic liquid crystals exhibit negative bend-splay elastic anisotropy[3–10] *i.e.*, $\delta K_{31} = K_{33} - K_{11} < 0$, giant flexoelectricity,[11–13] large rotational viscosity,[4,14–16] and biaxiality.[17–24] Since the free rotation of the molecules around the bow axis is hindered, BC molecules have a strong tendency to form nano-sized smectic clusters, known as cybotactic clusters.[3,25–31] The unusual properties, some of which are reported above, have been attributed to the effect of these clusters. The size of the stable smectic clusters has been measured experimentally using cryo-transmission electron microscopy (cryo-TEM).[32] These smectic clusters are expected to offer both bending modulus and layer compressional modulus which would impact the complex shear modulus of the nematic phase. However, measurements using conventional rheological techniques involving bulk samples would smear out their effect. Therefore, microrheological techniques, involving a very small amount of sample (typically a few microlitres), are important.[33]

In this paper, we report on the measurements of flow viscosities and the complex directional shear modulus and correlate the results with the splay and bend elastic constants of two asymmetric bent-core liquid crystals. Our study shows that microrheological approach using self-diffusing microparticles is a sensitive technique to investigate the cybotactic clusters in bent-core nematic (BCN) liquid crystals.

2 Materials and methods

2.1 Materials

Two homologous bent-core compounds, namely $8OCH_3$ and $16OCH_3$, with non-polar ($-OCH_3$) moieties were synthesized in our laboratory, where 8 and 16 represents the length of hydrocarbon chain R (see Fig. 1). The details of the synthesis were reported previously by us.[34] The chemical structures of the molecules and the phase transition temperatures of the compounds are shown in Fig. 1. They exhibit the following phase

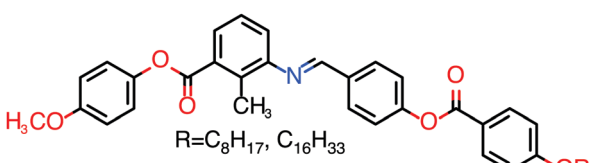

Fig. 1 Chemical structures of the asymmetric bent-core molecules and phase transition temperatures.

[a] *School of Physics, University of Hyderabad, Hyderabad, India. E-mail: sathyapaladugu@gmail.com, sdsp@uohyd.ernet.in*
[b] *Soft and Active Matter Group, Department of Physics, Indian Institute of Science Education and Research (IISER), Tirupati, Andhra Pradesh 517507, India*
[c] *Department of Chemical Sciences, Indian Institute of Science Education and Research (IISER) Mohali, Sector-81, Knowledge City, Manauli, 140306, India*

† Electronic supplementary information (ESI) available. See DOI: 10.1039/d0sm00796j

transitions in cooling: $8OCH_3$: I 150.1 °C N 66.7 °C Cr and $16OCH_3$: I 126.7 °C N 97.7 °C SmA 73.4 °C Cr.

2.2 Experimental

The experimental cells for aligning the liquid crystal director were prepared with two patterned indium-tin-oxide (ITO) coated glass plates. The ITO plates were spin coated with polyimide AL1254 and baked at 180 °C for 1 h. The AL1254 coated glass plates were then rubbed with a rubbing machine and assembled in an antiparallel way to ensure uniform planar alignment of the director. The glass plates were glued together with UV-curable adhesive (NOA65-Norland Products, Inc.) with silica beads as spacers. The thickness of the cells (d) was measured using an interferometric method and the typical cell thickness used in the study was 8 μm.

The dielectric constant as a function of voltage (0.02–20 V) at different temperatures in the nematic phase was measured at 4.111 kHz with an LCR meter (Agilent 4980A). The perpendicular component of the dielectric constant ($\varepsilon_\perp$) was obtained from the dielectric measurement below the Freedericksz threshold voltage (V_{th}) and the parallel component ($\varepsilon_\parallel$) was obtained by extrapolating the voltage dependent dielectric constant to $V \to \infty$, *i.e.*, $1/V \to 0$. Simultaneously, the voltage dependent optical retardation was measured with the help of a home built electrooptic setup, consisting of a photo-elastic modulator (Hinds Instruments) and a lock-in amplifier (SRS-830). The experimental diagram of the setup is shown in Fig. 2(a). From the Freedericksz threshold voltage (V_{th}) of the retardation measurement, the splay elastic constant (K_{11}) was obtained, using the relation $K_{11} = \varepsilon_0\Delta\varepsilon(V_{th}/\pi)^2$, where $\Delta\varepsilon = \varepsilon_\parallel - \varepsilon_\perp$ is the dielectric anisotropy. The bend elastic constant (K_{33}) was obtained by fitting the voltage dependent optical retardation, following the method described in ref. 35–37. The accuracy in the measurement of the elastic constant is within 6%.

The flow viscosities parallel ($\eta_\parallel$) and perpendicular ($\eta_\perp$) to the director were measured by measuring the self-diffusion of a silica particle of diameter 3 μm.[38,39] Before dispersing in LCs, the particles were treated with octadecyldimethyl(3-trimethoxysilylpropyl)ammonium chloride (DMOAP), which aligns the director normal to the surface.[40] Normal anchoring induces a point defect and stabilises a dipolar director field surrounding the particles, as a result of which the particles are levitated in the bulk due to elastic repulsion from the surface.[41] This is advantageous as a long duration (about several hours) of data collection is required. The dynamics of the Brownian motion of an isolated silica particle in the BCN was recorded through a 60× water immersion objective using a CCD camera (iDs-UI) connected to a Nikon inverted microscope with a frame rate of 20 fps.[42] The diagram of the experimental setup is shown in Fig. 2(b). The trajectory of a particle is extracted from the recorded sequence of images using a Python routine known as Trackpy.[43] The mean squared displacements (MSDs) parallel and perpendicular to the director were measured with the lag time τ. The diffusion coefficients parallel ($D_\parallel$) and perpendicular ($D_\perp$) to the director were measured from the respective MSDs as a function of the lag time τ, using the equations $\langle(x(t+\tau) - x(t))^2\rangle = 2D_\parallel\tau$ and $\langle(y(t+\tau) - y(t))^2\rangle = 2D_\perp\tau$. The corresponding viscosities are calculated using the Stokes–Einstein equation, $\eta_{\parallel,\perp} = k_BT/6\pi RD_{\parallel,\perp}$, where k_B is the Boltzmann constant, T is the absolute temperature and R is the radius of the microparticle.[40]

The complex viscoelastic shear modulus $G^*(\omega) = G'(\omega) + iG''(\omega)$, where $G'(\omega)$ is the storage modulus and $G''(\omega)$ is the loss modulus in the frequency (ω) domain, was calculated using the generalized Stokes–Einstein equation (GSER).[44] The GSER in the Fourier domain can be expressed as:

$$G^*(\omega) = G'(\omega) + iG''(\omega) = \frac{k_BT}{\pi Ri\omega\mathcal{F}\{<\Delta r^2(t)>\}} \quad (1)$$

where $\mathcal{F}$ denotes the Fourier transform and R is the radius of the microparticle. The parallel ($G_\parallel^*(\omega)$) and perpendicular components ($G_\perp^*(\omega)$) of the complex shear modulus $G^*(\omega)$ were obtained from the mean squared displacement (MSD) parallel and perpendicular to the nematic director by the equations $G_\parallel^*(\omega) = \frac{k_BT}{2\pi Ri\omega\mathcal{F}\{<\Delta x^2(t)>\}}$ and $G_\perp^*(\omega) = \frac{k_BT}{2\pi Ri\omega\mathcal{F}\{<\Delta y^2(t)>\}}$, respectively.[45]

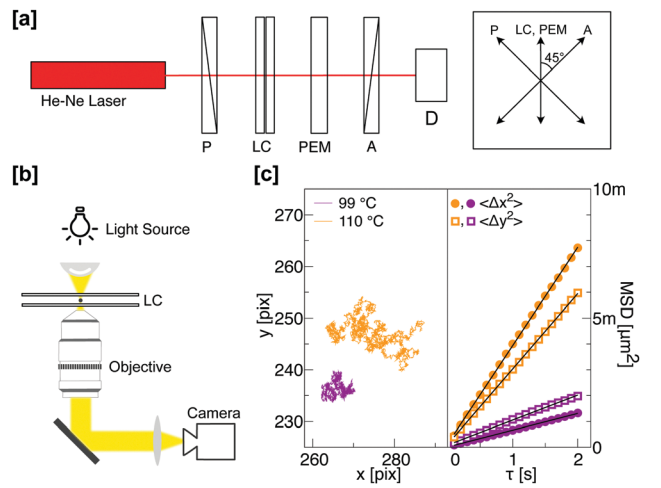

Fig. 2 (a) Schematic diagram of the experimental setup for measuring birefringence, and splay and bend elastic constants. (b) Setup for microrheological studies. (c) Trajectories and time evolution of the MSD (mean squared displacement) of a microparticle at 99 °C and 110 °C of compound $16OCH_3$. The diffusion coefficients $D_\parallel$, $D_\perp$ at 110 °C and 99 °C (in 10^{-15} m^2 s^{-1}) are 1.90, 1.46 and 0.32, 0.48, respectively.

3 Results and discussion

3.1 Splay and bend elastic constants

We begin with the discussion of the splay (K_{11}) and bend (K_{33}) elastic constants of the compounds. Both the compounds exhibit positive birefringence (Δn) and dielectric anisotropy ($\Delta\varepsilon$) (see the ESI†). The temperature dependence of K_{11} and K_{33} of both the compounds is shown in Fig. 3(a) and (b). The bend-splay anisotropy ($\delta K_{31} = K_{33} - K_{11}$) of compound $8OCH_3$ is negative in the entire nematic range and its magnitude continues

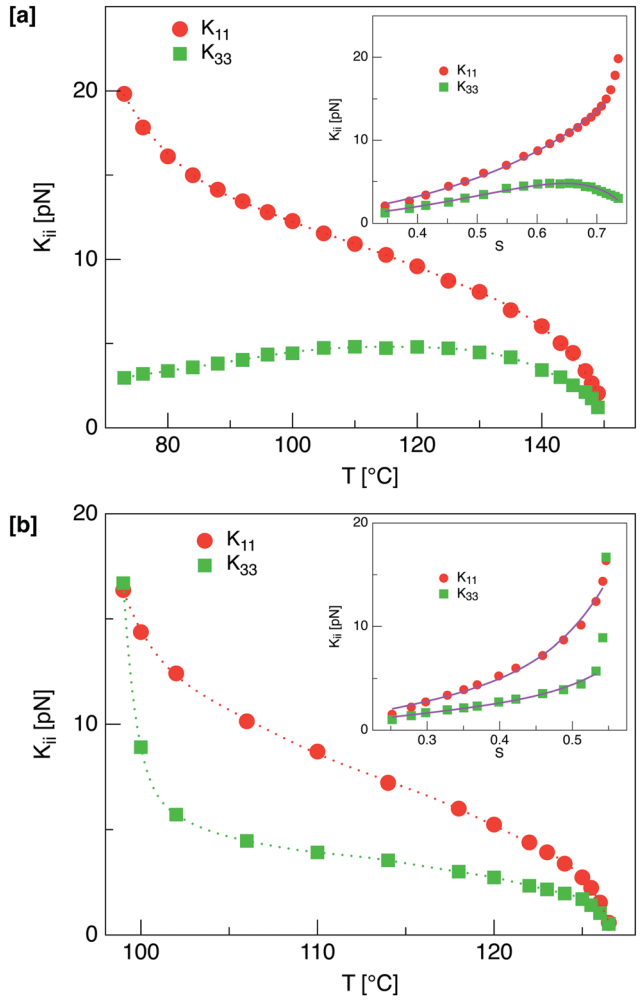

Fig. 3 (a) Temperature dependent splay (K_{11}) and bend (K_{33}) elastic constants of $8OCH_3$. (Inset) K_{ii} as a function of order parameter S. (b) Temperature dependent K_{11} and K_{33} of $16OCH_3$. (Inset) K_{ii} as a function of order parameter S. Continuous lines are theoretical fits to eqn (2).

to increase with decreasing temperature. Similar negative anisotropy has been reported in many symmetric and asymmetric bent-core nematic liquid crystals.[8,10,15,46] The negative anisotropy is attributed to the coupling of the bent-shape of the molecules with the bend distortion.[3] For most of the liquid crystals made of rod-like molecules, $K_{ii} \propto S^2$, where S is the orientational order parameter. To see how K_{ii} of these compounds depends on the order parameter, we plot K_{ii} as a function of S as shown in the inset of Fig. 3(a). The order parameter S was obtained from the temperature dependent birefringence (ESI†). It is noticed that K_{33} shows antagonistic dependence on the order parameter and simply can not be fitted to second-order in S. In particular, K_{33} of $16OCH_3$ tends to decrease after a pronounced maximum. The dependence of K_{ii} on S could be better explained using more detailed mean-field calculations given by Berreman and Meiboom.[47] They introduce a third-order dependence on S given by:

$$K_{ii} = K_i^{(2)} S^2 + K_i^{(3)} S^3 + K_i^{(4)} \frac{S^4}{(1-S)^2} \qquad (2)$$

where K_i^n, $n = 2, 3, 4$ are fitting parameters. The continuous line in the inset of Fig. 3(a) is a theoretical fit to eqn (2). Considering that the $K_i^{(2)-(4)}$s are temperature independent, the fitting parameters (measured in pN) for $8OCH_3$ are found to be: $K_1^{(2)} = 14.3 \pm 1.1$, $K_1^{(3)} = 13.7 \pm 1.2$, $K_1^{(4)} = 0.7 \pm 0.1$, and $K_3^{(2)} = 6.4 \pm 1.1$, $K_3^{(3)} = 17.2 \pm 1.2$, $K_3^{(4)} = -1.8 \pm 0.1$.

The temperature dependence of K_{11} and K_{33} of compound $16OCH_3$ is shown in Fig. 3(b). In this compound, the bend-splay anisotropy, $\delta K_{31} = K_{33} - K_{11}$, is also negative, except very close to the N–SmA phase transition temperature. In particular, as the N–SmA transition is approached, δK_{31} tends to change sign from negative to positive. This feature is explained by the strong pre-transitional divergence of K_{33} as the bend deformation is incompatible with the equidistance of smectic layers. The dependence of K_{ii} on S is shown in the inset of Fig. 3(b). Excellent fits are obtained with the fit-parameters for $16OCH_3$ (measured in pN): $K_1^{(2)} = 46.5 \pm 1.1$, $K_1^{(3)} = -67.5 \pm 1.2$, $K_1^{(4)} = 26.3 \pm 0.1$ and $K_3^{(2)} = 30.9 \pm 1.1$, $K_3^{(3)} = -48.1 \pm 1.2$, $K_3^{(4)} = 10.8 \pm 0.1$.

3.2 Flow viscosities

In what follows we measured the flow viscosities of these compounds from the self-diffusion of microparticles following the technique described in Section 2.2. The measurements are restricted only to the nematic phase as the particles tend to sediment quickly in the isotropic phase. Some representative trajectories of a microparticle and corresponding MSDs at two temperatures, namely 99 °C and 110 °C, for compound $16OCH_3$ are shown in Fig. 2(c). It is found that at 110 °C, $D_{||}/D_{\perp} \simeq 1.3$, whereas at 99 °C, which is very close to the N–SmA transition temperature, $D_{||}/D_{\perp} \simeq 0.7$.

The temperature dependent viscosities parallel and perpendicular to the director, namely $\eta_{\parallel}$ and $\eta_{\perp}$, of compound $8OCH_3$ below the isotropic to nematic transition temperature (T_{NI}) are shown in the inset of Fig. 4. Both $\eta_{\parallel}$ and $\eta_{\perp}$ increase with decreasing temperature as expected. In the entire nematic range $\eta_{\perp} > \eta_{\parallel}$, thus the viscosity anisotropy ($\delta\eta = \eta_{\perp} - \eta_{\parallel}$) is positive. For example, at a temperature $T = 70$ °C, $\delta\eta = \eta_{\perp} - \eta_{\parallel} \simeq 100$ mPa s.

The temperature dependent viscosities of compound $16OCH_3$ in the nematic phase are shown in Fig. 4. Both $\eta_{\parallel}$ and $\eta_{\perp}$ increase with decreasing temperature as expected. However, the rate of increase of the viscosities at lower temperatures of $16OCH_3$ is much faster than that of $8OCH_3$. This is expected due to the increasing amplitude of fluctuations in smectic order as the N–SmA transition is approached, similar to those observed in ordinary rod-like LCs showing the same transition. Interestingly, it is found that for $16OCH_3$, below $T \approx 104$ °C, $\delta\eta$ changes sign from positive to negative. For example, at $T = 114$ °C, $\delta\eta \simeq 40$ mPa s, whereas at $T = 98$ °C, $\delta\eta \simeq -110$ mPa s. The sign change of the anisotropy can not simply be explained based on the presmectic fluctuations as that would affect both the viscosities equally. We attribute this effect to the cybotactic clusters of compound $16OCH_3$. These clusters are stable compared to the unstable clusters in ordinary liquid crystals with rod-like molecules as the free rotation of the former around the bow axis is reduced sufficiently due to the steric hindrance. Moreover, the size and the

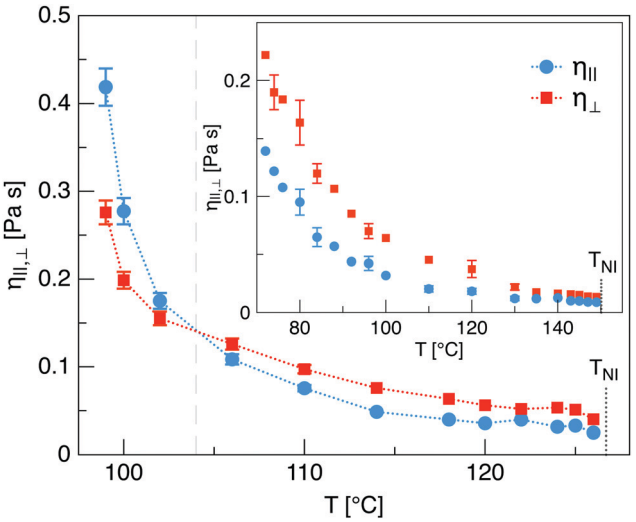

Fig. 4 Temperature dependent flow viscosities parallel ($\eta_{||}$) and perpendicular ($\eta_{\perp}$) to the director of 16OCH$_3$. (Inset) Temperature dependent $\eta_{||}$ and $\eta_{\perp}$ of 8OCH$_3$. Error bars represent the standard deviation of the mean value. T_{NI} indicates the isotropic to nematic phase transition temperature.

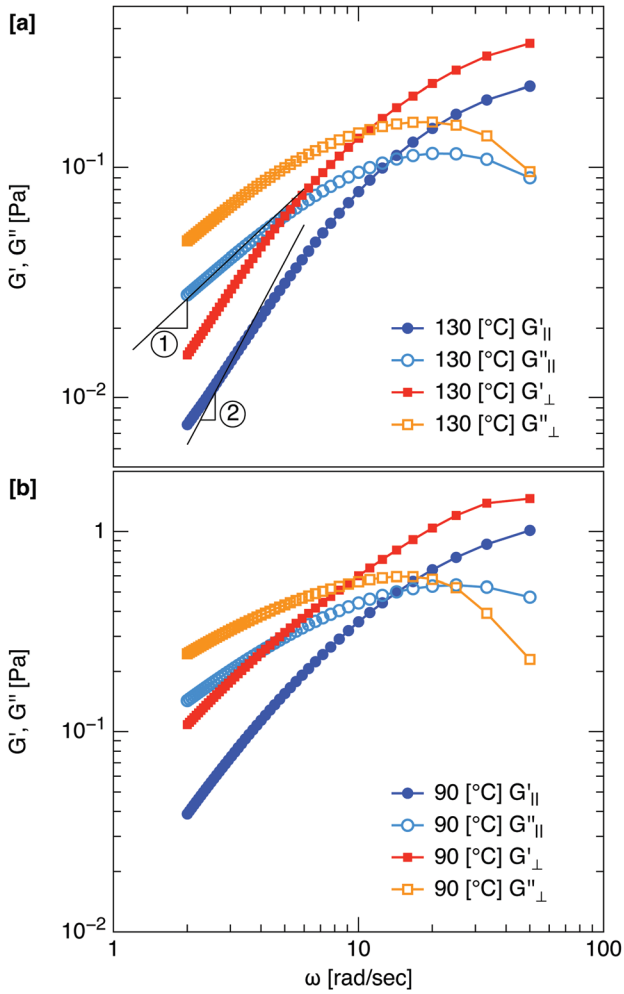

Fig. 5 Frequency dependent storage ($G'(\omega)$) and loss modulus ($G''(\omega)$) of 8OCH$_3$. The subscripts || and ⊥ denote the components parallel and perpendicular to the director at (a) 130 °C and (b) 90 °C. ① and ② represent the exponents of ω corresponding to the loss and storage moduli, respectively, in the Maxwell-fluid model.

volume fraction of these clusters near the N to SmA transition are expected to grow. The resulting smectic planes of the clusters are oriented perpendicular to the director in a planar cell. These oriented clusters effectively reduce the self-diffusion of the microparticle parallel to the director (perpendicular to the smectic planes) compared to the perpendicular direction (parallel to the smectic planes), resulting in negative viscosity anisotropy. Further comparative studies on cluster size and stability between bent-core and ordinary rod-like LCs exhibiting an N–SmA transition could be reassuring.

3.3 Complex shear modulus

The temperature dependent elastic constants and flow viscosities demonstrated the presence of stable cybotactic clusters in the nematic phase of compound 16OCH$_3$ that contributes greatly to these properties, especially near the N to SmA phase transition. As a next step, we investigate the effect of these clusters on the complex shear modulus $G^*(\omega)$. Fig. 5 and 6 show the frequency dependence of the storage ($G_{||}'(\omega)$ and $G_{\perp}'(\omega)$) and loss modulus ($G_{\parallel}''(\omega)$ and $G_{\perp}''(\omega)$) parallel and perpendicular to the nematic director at two different temperatures. Overall, both the parallel and perpendicular components exhibit fluid-like behaviour: a storage modulus lower than the corresponding loss modulus below a critical frequency. In the low frequency range one observes a behaviour typical of a Maxwell-fluid: $G_{\parallel,\perp}''(\omega) \propto \omega$ and $G_{\parallel,\perp}'(\omega) \propto \omega^2$ (see Fig. 5(a) and 6(a)).

In the nematic phase of 8OCH$_3$ the perpendicular components are greater than the corresponding parallel components, *i.e.*, $G_{\perp}'(\omega) > G_{||}'(\omega)$ and $G_{\perp}''(\omega) > G_{\parallel}''(\omega)$ (see Fig. 5(a) and (b)). Similar behaviour is also seen in compound 16OCH$_3$ at T = 120 °C (Fig. 6(a)). However, at lower temperature (T = 100 °C), just above the N–SmA transition temperature, the trend is quite opposite when the relative magnitudes of the parallel and perpendicular components are compared. In particular, $G_{||}'(\omega) > G_{\perp}'(\omega)$ and also $G_{\parallel}''(\omega) > G_{\perp}''(\omega)$ (see Fig. 6(b)), which is just opposite to the behaviour seen at higher temperature (T = 120 °C). In addition, the magnitudes of the directional moduli at T = 100 °C are almost one order of magnitude larger than those measured at T = 120 °C. To bring out the contrasting behaviour we show the ratios $G_{\parallel}'(\omega)/G_{\perp}'(\omega)$ and $G_{\parallel}''(\omega)/G_{\perp}''(\omega)$ at a fixed ω (2 rad s^{-1}) in Tables 1 and 2. In compound 8OCH$_3$, at two different temperatures $G_{\parallel}'(\omega)/G_{\perp}'(\omega) < 1$ and also $G_{\parallel}''(\omega)/G_{\perp}''(\omega) < 1$ (Table 1). For compound 16OCH$_3$ at higher temperature (T = 120 °C), both the ratios are also less than 1 (Table 2). However, at lower temperature (T = 100 °C), $G_{\parallel}'(\omega)/G_{\perp}'(\omega) > 1$ and $G_{\parallel}''(\omega)/G_{\perp}''(\omega) > 1$, which are opposite to the features observed at T = 120 °C. Thus, the parallel components of the complex viscoelastic shear modulus of 16OCH$_3$ exceed the perpendicular components just above the N–SmA phase transition temperature.

This distinct feature in the nematic phase can be explained considering the contribution of stable cybotactic clusters.

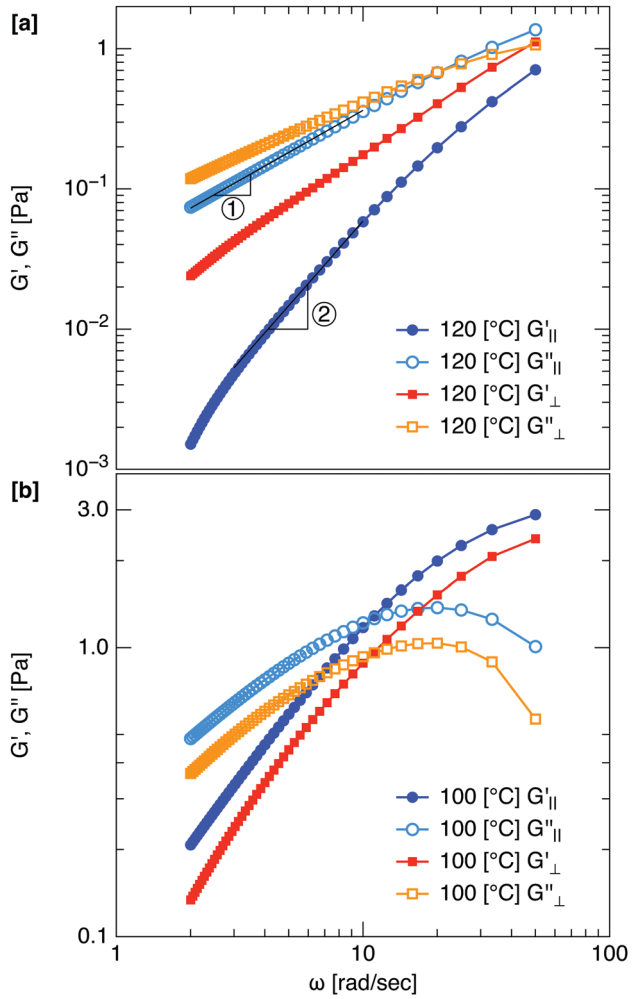

Fig. 6 Frequency dependent storage ($G'(\omega)$) and loss modulus ($G''(\omega)$) of $16OCH_3$. The subscripts || and ⊥ denote the components parallel and perpendicular to the director at (a) 120 °C and (b) 100 °C. ① and ② represent the exponents of ω corresponding to the loss and storage moduli, respectively, in the Maxwell-fluid model.

Table 1 Ratio of the real and imaginary components parallel and perpendicular to the director of compound $8OCH_3$ at ω = 2 [rad s^{-1}]

Temp. [°C]	$G_{\parallel}'(\omega)/G_{\perp}'(\omega)$	$G_{\parallel}''(\omega)/G_{\perp}''(\omega)$
130	0.5	0.6
90	0.3	0.6

Table 2 Ratio of the real and imaginary components parallel and perpendicular to the director of compound $16OCH_3$ at ω = 2 [rad s^{-1}]

Temp. [°C]	$G_{\parallel}'(\omega)/G_{\perp}'(\omega)$	$G_{\parallel}''(\omega)/G_{\perp}''(\omega)$
120	0.1	0.6
100	1.5	1.3

In analogy with smectic droplets, the storage modulus of the cybotactic clusters can be written as $G' = C\sqrt{(KB/L)}$ where K is the bending modulus, B is the layer compressional modulus, L is the cluster size and C is a constant.[48,49] At higher temperature (near the NI transition) the clusters are unstable and consequently the contribution due to the layer compressional modulus B is negligible. As the temperature is reduced towards the N–SmA transition, the clusters become stable and their size and the volume fraction increase,[50] as a result of which G' is enhanced. Taking G' = 2 Pa (Fig. 6(b)), K = 5 pN (Fig. 3(b)), $C \approx 0.2$[49] and assuming a typical layer compressional modulus $B \approx 10^6$ Pa,[51] the calculated cluster size $L \approx 50$ nm, which is very close to the size measured by cryo-transmission electron microscopy (cryo-TEM) in similar bent-core liquid crystals.[32]

4 Conclusions

In conclusion, we studied the elastic properties, flow viscosities and directional shear modulus of two bent-core liquid crystals. The bend-splay anisotropy ($\delta K_{31} = K_{33} - K_{11}$) of compound $8OCH_3$ is negative at all temperatures, whereas, for $16OCH_3$, δK_{31} tends to change sign just above the SmA–N transition temperature. For compound $8OCH_3$, the flow viscosity anisotropy $\delta\eta = (\eta_{\perp} - \eta_{||}) > 0$ at all temperatures. In the case of $16OCH_3$ it changes sign just above the SmA–N phase transition temperature. The parallel components of the complex shear modulus of compound $16OCH_3$ exceed the perpendicular components, just above the N–SmA phase transition temperature. This special feature is explained considering the contribution of the layer compressional modulus of stable smectic clusters in the nematic phase. Our experiment provided an approximate estimate of the size of the smectic clusters which is comparable to the size measured by using the cryo-TEM. The microrheology experiments require a few microlitres of sample and can be used for probing the effects of nanoscale heterogeneity due to short-range order in liquid crystals and in other soft materials.

Conflicts of interest

There are no conflicts to declare.

Acknowledgements

SD acknowledges financial support from SERB (Ref. No. CRG/2019/000425) and DST-FIST-II, School of Physics. SKP thanks SERB (file no. CRG/2019/000901/OC) for funding. SP thanks IISER Tirupati for the fellowship and research support. RKP acknowledges Department of Science and Technology, India, for INSPIRE Faculty award grant DST/INSPIRE/04/2016/002370. SK acknowledges IISER Mohali for a PhD fellowship. GM acknowledges DST-SERB, India, for NPDF File No. (NPDF/2016/000560).

Notes and references

1 H. Takezoe and Y. Takanishi, *Jpn. J. Appl. Phys.*, 2006, **45**, 597–625.
2 A. Jákli, O. D. Lavrentovich and J. V. Selinger, *Rev. Mod. Phys.*, 2018, **90**, 045004.

3 P. Sathyanarayana, M. Mathew, Q. Li, V. S. S. Sastry, B. Kundu, K. V. Le, H. Takezoe and S. Dhara, *Phys. Rev. E: Stat., Nonlinear, Soft Matter Phys.*, 2010, **81**, 010702.
4 P. Sathyanarayana, S. Radhika, B. K. Sadashiva and S. Dhara, *Soft Matter*, 2012, **8**, 2322–2327.
5 V. Görtz, C. Southern, N. W. Roberts, H. F. Gleeson and J. W. Goodby, *Soft Matter*, 2009, **5**, 463–471.
6 P. Tadapatri, U. S. Hiremath, C. V. Yelamaggad and K. S. Krishnamurthy, *J. Phys. Chem. B*, 2010, **114**, 1745–1750.
7 M. Majumdar, P. Salamon, A. Jákli, J. T. Gleeson and S. Sprunt, *Phys. Rev. E: Stat., Nonlinear, Soft Matter Phys.*, 2011, **83**, 031701.
8 S. Kaur, J. Addis, C. Greco, A. Ferrarini, V. Görtz, J. W. Goodby and H. F. Gleeson, *Phys. Rev. E: Stat., Nonlinear, Soft Matter Phys.*, 2012, **86**, 041703.
9 S. Kaur, G. Mohiuddin, P. Satapathy, R. Nandi, V. Punjani, S. K. Prasad and S. K. Pal, *Mol. Syst. Des. Eng.*, 2018, **3**, 839–852.
10 N. Avci, V. Borshch, D. D. Sarkar, R. Deb, G. Venkatesh, T. Turiv, S. V. Shiyanovskii, N. V. S. Rao and O. D. Lavrentovich, *Soft Matter*, 2013, **9**, 1066–1075.
11 J. Harden, B. Mbanga, N. Éber, K. Fodor-Csorba, S. Sprunt, J. T. Gleeson and A. Jákli, *Phys. Rev. Lett.*, 2006, **97**, 157802.
12 P. Sathyanarayana and S. Dhara, *Phys. Rev. E: Stat., Nonlinear, Soft Matter Phys.*, 2013, **87**, 012506.
13 K. V. Le, F. Araoka, K. Fodor-Csorba, K. Ishikawa and H. Takezoe, *Liq. Cryst.*, 2009, **36**, 1119–1124.
14 P. Sathyanarayana, T. A. Kumar, V. S. S. Sastry, M. Mathews, Q. Li, H. Takezoe and S. Dhara, *Appl. Phys. Express*, 2010, **3**, 091702.
15 P. Sathyanarayana, V. S. R. Jampani, M. Skarabot, I. Musevic, K. V. Le, H. Takezoe and S. Dhara, *Phys. Rev. E: Stat., Nonlinear, Soft Matter Phys.*, 2012, **85**, 011702.
16 E. Dorjgotov, K. Fodor-Csorba, J. T. Gleeson, S. Sprunt and A. Jákli, *Liq. Cryst.*, 2008, **35**, 149–155.
17 J. A. Olivares, S. Stojadinovic, T. Dingemans, S. Sprunt and A. Jákli, *Phys. Rev. E: Stat., Nonlinear, Soft Matter Phys.*, 2003, **68**, 041704.
18 B. R. Acharya, A. Primak and S. Kumar, *Phys. Rev. Lett.*, 2004, **92**, 145506.
19 L. A. Madsen, T. J. Dingemans, M. Nakata and E. T. Samulski, *Phys. Rev. Lett.*, 2004, **92**, 145505.
20 Y. Jang, V. P. Panov, A. Kocot, J. K. Vij, A. Lehmann and C. Tschierske, *Appl. Phys. Lett.*, 2009, **95**, 183304.
21 Y. Xiang, J. W. Goodby, V. Görtz and H. F. Gleeson, *Appl. Phys. Lett.*, 2009, **94**, 193507.
22 M. Lehmann, *Liq. Cryst.*, 2011, **38**, 1389–1405.
23 H. Yoon, S.-W. Kang, M. Lehmann, J. O. Park, M. Srinivasarao and S. Kumar, *Soft Matter*, 2011, **7**, 8770–8775.
24 T. B. T. To, T. J. Sluckin and G. R. Luckhurst, *Phys. Rev. E: Stat., Nonlinear, Soft Matter Phys.*, 2013, **88**, 062506.
25 S. Stojadinovic, A. Adorjan, S. Sprunt, H. Sawade and A. Jákli, *Phys. Rev. E: Stat., Nonlinear, Soft Matter Phys.*, 2002, **66**, 060701.
26 P. Sathyanarayana, B. K. Sadashiva and S. Dhara, *Soft Matter*, 2011, **7**, 8556–8560.
27 C. Tschierske and D. J. Photinos, *J. Mater. Chem.*, 2010, **20**, 4263–4294.
28 R. Y. Dong, *Int. J. Mod. Phys. B*, 2010, **24**, 4641–4682.
29 C. Keith, A. Lehmann, U. Baumeister, M. Prehm and C. Tschierske, *Soft Matter*, 2010, **6**, 1704–1721.
30 O. Francescangeli and E. T. Samulski, *Soft Matter*, 2010, **6**, 2413–2420.
31 V. Domenici, *Soft Matter*, 2011, **7**, 1589–1598.
32 C. Zhang, M. Gao, N. Diorio, W. Weissflog, U. Baumeister, S. Sprunt, J. T. Gleeson and A. Jákli, *Phys. Rev. Lett.*, 2012, **109**, 107802.
33 C. Bailey, K. Fodor-Csorba, J. T. Gleeson, S. N. Sprunt and A. Jákli, *Soft Matter*, 2009, **5**, 3618–3622.
34 S. Kaur, G. Mohiuddin, V. Punjani, R. K. Khan, S. Ghosh and S. K. Pal, *J. Mol. Liq.*, 2019, **295**, 111687.
35 H. J. Deuling, *Mol. Cryst. Liq. Cryst.*, 1972, **19**, 123–131.
36 H. Gruler, T. J. Scheffer and G. Meier, *Z. Naturforsch., A: Phys., Phys. Chem., Kosmophys.*, 1972, **27**, 966.
37 G. Barbero and L. R. Evangelista, *An Elementary Course on the Continuum Theory for Nematic Liquid Crystals*, World Scientific, 2000.
38 J. C. Loudet, P. Hanusse and P. Poulin, *Science*, 2004, **306**, 1525.
39 H. Stark, *Phys. Rep.*, 2001, **351**, 387–474.
40 M. Škarabot and I. Muševič, *Soft Matter*, 2010, **6**, 5476–5481.
41 O. P. Pishnyak, S. Tang, J. R. Kelly, S. V. Shiyanovskii and O. D. Lavrentovich, *Phys. Rev. Lett.*, 2007, **99**, 127802.
42 J. C. Crocker and D. G. Grier, *J. Colloid Interface Sci.*, 1996, **179**, 298–310.
43 D. Allan, C. van der Wel, N. Keim, T. A. Caswell, D. Wieker, R. Verweij, C. Reid, Thierry, L. Grueter, K. Ramos, apiszcz, zoeith, R. W. Perry, F. Boulogne, P. Sinha, pfigliozzi, N. Bruot, L. Uieda, J. Katins, H. Mary and A. Ahmadia, *soft-matter/trackpy: Trackpy v0.4.2*, 2019, DOI: 10.5281/zenodo.3492186.
44 T. G. Mason, K. Ganesan, J. H. van Zanten, D. Wirtz and S. C. Kuo, *Phys. Rev. Lett.*, 1997, **79**, 3282–3285.
45 J. He, M. Mak, Y. Liu and J. X. Tang, *Phys. Rev. E: Stat., Nonlinear, Soft Matter Phys.*, 2008, **78**, 011908.
46 B. Kundu, R. Pratibha and N. V. Madhusudana, *Phys. Rev. Lett.*, 2007, **99**, 247802.
47 D. W. Berreman and S. Meiboom, *Phys. Rev. A: At., Mol., Opt. Phys.*, 1984, **30**, 1955–1959.
48 P. Panizza, D. Roux, V. Vuillaume, C.-Y. D. Lu and M. E. Cates, *Langmuir*, 1996, **12**, 248–252.
49 S. Fujii, S. Komura, Y. Ishii and C.-Y. D. Lu, *J. Phys.: Condens. Matter*, 2011, **23**, 235105.
50 Y. P. Panarin, S. P. Sreenilayam, J. K. Vij, A. Lehmann and C. Tschierske, *Beilstein J. Nanotechnol.*, 2018, **9**, 1288.
51 M. Benzekri, T. Claverie, J. P. Marcerou and J. C. Rouillon, *Phys. Rev. Lett.*, 1992, **68**, 2480–2483.